PAPER

Check for updates

A sensitive BODIPY-based fluorescent probe for detecting endogenous hydroxyl radicals in living cells†

Xingyu Qu, [ID] Yongjun Bian, [ID]* Yongqiang Chen* and Xiaoqing Wei

The hydroxyl radical (˙OH) has been suggested to play very vital roles in many physiological and pathological processes. However, selective detection of ˙OH is highly challenging owing to its extremely high reactivity and short lifetime. Herein, we designed and synthesized a sensitive "turn on" fluorescent probe for detecting endogenous ˙OH based on a BODIPY (4,4-difluoro-4-bora-3*a*,4*a*-diaza-*s*-indacene) platform. The probe had shown good properties including high sensitively, ideal selectively and low cytotoxicity, and was successfully employed to image endogenous hydroxyl radical in living cells.

Introduction

The hydroxyl radical (˙OH), an unstable and highly reactive molecule, has aroused growing attention in the past decades. It has been widely used in many areas of human health, including drinking water treatment,[1–3] air quality monitoring,[4] cancer treatment,[5] *etc.* Normal levels of ˙OH in cells play critical roles in regulating many physiological and pathological events. However, excessive ˙OH is extremely harmful to human health and leads to a series of physiological diseases like aging and Parkinson's disease by reacting with numerous biomacromolecules including DNA bases, lipids, and proteins.[6] Therefore, rapid, sensitive and accurate detection of intracellular ˙OH concentration is of vital importance in order to well understand its biological impact and timely hamper its damage. Whereas, selectively monitoring ˙OH is very difficult due to its short life-time (about 10^{-9} s).

For ˙OH detection, many analytic methods have been applied, such as electron spin resonance spectroscopy,[7,8] chromatography,[9] chemiluminescence[10,11] and electrochemistry.[12–14] Nevertheless, most of them either require expensive instruments or are not sensitive enough towards ˙OH and not suitable for monitoring ˙OH in live cells. By comparison, fluorescence-based ways might be a better choice because of these prominent advantages like simplicity, high sensitivity, high-speed spatial analysis, low bio-damaging, real-time monitoring in live cells, *etc.* Indeed, several fluorescence probes have been developed during the past few years, for instance, organic small molecules,[15–20] semiconductor quantum dots[21–23] and metal nanoclusters.[24] Among them, the fluorescence probes based on

College of Chemistry and Chemical Engineering, Jinzhong University, Yuci 030619, China. E-mail: yjbian2013@jzxy.edu.cn; chenyongqiang@jzxy.edu.cn

† Electronic supplementary information (ESI) available. See DOI: 10.1039/d0ra05378c

organic small molecules are one of the most successful species owing to easily modified, high sensitive and nontoxic or low toxic. As one of the important organic fluorophores, 4,4-difluoro-3*a*,4*a*-diaza-*s*-indacene (BODIPY) with relatively high fluorescence quantum yields, high extinction coefficient and good photostability, have drawn increasing attention.[25–31]

To construct high sensitive and selective probes for detecting hydroxyl radical, a general strategy is to conjugate an organic fluorescence molecule with a recognition element moiety for specifically trapping and reacting with ˙OH. For example, Wang *et al.* reported a BODIPY probe with *gem*-dichloro moiety reacting with ˙OH *via* a substitute reaction and showed good selectivity and biocompatibility for cellar imaging of hydroxyl radical in live cells.[32] The oxidation potential of ˙OH is around 2.8 eV (ref. 3) and high enough to oxidize Ph₃P (the reduction electrode potential is 2.7 eV) to Ph₃P=O. But other reactive oxygen species (ROS), such as H_2O_2, $O_2{}^{\cdot-}$, ClO^-, are failure for this oxidation process. Based on this mechanism, a high selective and biocompatible BODIPY probe with Ph₃P moieties was reported by our group in 2018.[33] Herein, on the basis of above work, we continually designed and synthesized a novel "turn-on" NIR fluorescent probe for monitoring ˙OH with a much improved solubility in aqueous solution, which also showed high selectivity toward ˙OH over other reactive oxygen/nitrogen species (ROS/RNS) and has been successfully applied to detect ˙OH for imaging in living cells.

## Results and discussion

Design and synthesis of the probe 1 and compound OX-1

The synthesis of probe **1** was accomplished through a three-step route depicted in Scheme 1. 3,4-Dihydroxybenzaldehyde was alkylated with 1-bromohexadecane to afford compound **3**. Compound **3** reacted with 2,4-dimethyl-pyrrole to generate compound **2** in moderate yield. The target fluorescent probe **1**
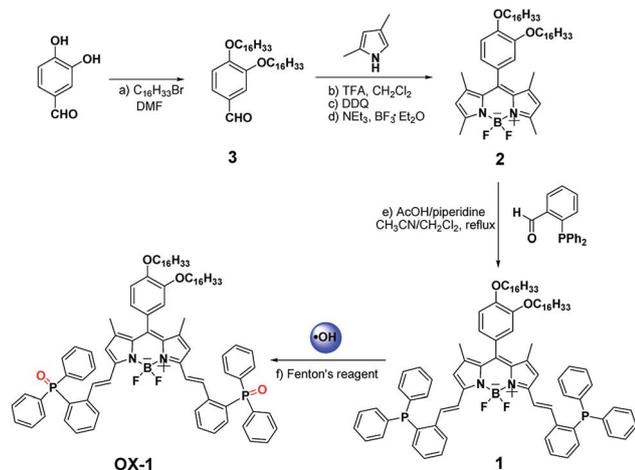
Scheme 1 Synthetic routes for the preparation of probe **1** and compound **OX-1**. (a) $C_{16}H_{33}Br$, K_2CO_3, KI, in DMF; (b) 2,4-dimethyl-pyrrole and trifluoroacetic acid in CH_2Cl_2; (c) DDQ; (d) triethylamine, $BF_3 \cdot OEt_2$; (e) 2-(diphenylphosphino)benzaldehyde, AcOH, piperidine; (f) Fenton's reagent.

Fig. 1 UV-Vis absorption (black line) and fluorescence spectra (red line) of probe **1** (10 µmol L^{-1}) in CH_2Cl_2 solvent.

was prepared by Knoevenagel condensation of compound **2** and 2-(diphenylphosphino)benzaldehyde. Compound **OX-1** was synthesized by Fenton reaction with probe **1**. Both probe **1** and compound **OX-1** were characterized by MALDI-TOF MS, ^{1}H NMR, ^{13}C NMR and ^{31}P NMR.

Spectral properties of the probe 1 and compound OX-1

The probe **1** based on BODIPY dyes using triphenylphosphine as a reactive-site tends to show good fluorescence properties and potential sensing application for detecting ˙OH. Hence, with the probe **1** and compound **OX-1** in hand, their spectral properties were firstly examined. The photo-physical properties of probe **1** and compound **OX-1** in various solvents were investigated at ambient temperature and summarized in Tables 1 and S1,† and the UV/Vis absorption and emission spectra of probe **1** in CH_2Cl_2 solvent were showed in Fig. 1. Probe **1** could be completely dissolved in organic solvents and the absorption spectra were slightly varied with increasing the solvent polarities. The absorption band of probe **1** was centered at 630 nm, 570 nm and 349 nm, and exciting at 580 nm, strong emissions typical for the BODIPY fluorescence dyes was observed at 650 nm. Compared with these of probe **1**, the photo-physical
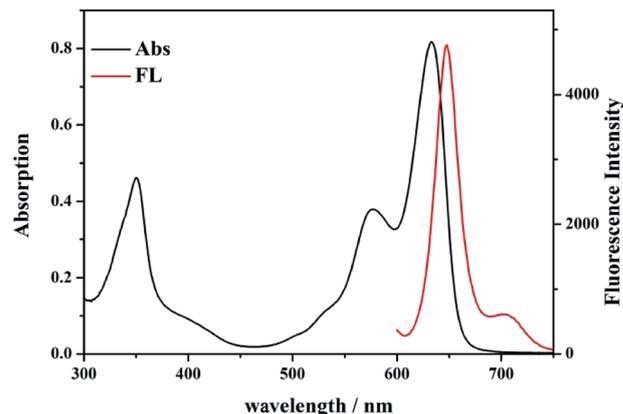
properties of the compound **OX-1** were similar, except the fluorescence quantum yield. The fluorescence quantum yield of probe **1** was 0.26 in dimethyl sulfoxide (DMSO) and about 0.67 in other organic solvents. Whereas, the fluorescence quantum yield of compound **OX-1** was above 0.62 in all organic solvents. These results indicated that probe **1** with high molar extinction coefficient probably can be used as a turn-on fluorescence sensor for monitoring ˙OH.

Fluorescence detection and selectivity of probe 1

The good fluorescence properties of probe **1** suggest it promising potential as fluorescence sensors. The fluorescence responses of probe **1** with ROS/RNS radicals were investigated in DMSO solution as shown in Fig. 2. Upon addition of ˙OH (0.1 mmol L^{-1}), the fluorescence intensity of probe **1** at 650 nm increased remarkably. The addition of a series of different ROS/RNS radicals (1.2 mmol L^{-1}), such as H_2O_2, ClO^-, $O_2^{˙-}$, TBHP, NO, NO_2^-, Vc, Fe^{3+}, GSH, respectively, did not generate similar enhancement and nearly unchanged. The above results demonstrated that its ˙OH response was not interfered in the background containing appropriate ROS/RNS radicals.

The titration experiments were also carried out to further assess the sensing ability of probe **1** towards ˙OH. The sensing process was operated by gradually increasing ˙OH concentration in the DMSO solution containing the probe **1** (10 µmol L^{-1}) as shown in Fig. 3. After adding ˙OH from 0 to 5 equivalent, the

Table 1 Optical properties of **1** and **OX-1** in CH_2Cl_2 and DMSO solvents at 298 K

Compounds	Solvents	λ_{abs}^{max} (nm)/log ε_{max}	λ_{flu} (nm)	$\Delta\lambda_{1/2}{}^a$ [nm]	$\Phi_f{}^b$	$\tau_f{}^c$ (nm)
1	CH_2Cl_2	633/4.93, 574/4.52, 349/4.68	650	29	0.67	4.68
	DMSO	628/4.93, 581/4.56	650	30	0.26	—
OX-1	CH_2Cl_2	630/4.92, 574/4.53, 355/4.70	646	27	0.63	4.24
	DMSO	630/4.92, 577/4.53	647	26	0.62	—

[a] Half width at maximum height. [b] Fluorescence quantum yield. [c] Fluorescence lifetimes.
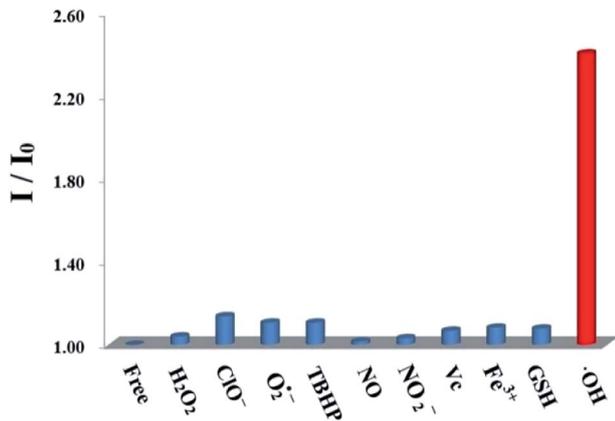
Fig. 2 Fluorescence reactivity of probe 1 (10 μmol L^{-1} in DMSO) with various ROS/RNS species (0.1 mmol L^{-1} of ˙OH, 1.2 mmol L^{-1} of H_2O_2, ClO$^-$, $O_2^{˙-}$, TBHP, NO, NO_2^-, Vc, Fe^{3+}, GSH) upon excitation at 580 nm. I and I_0 were the fluorescence intensity of the probe in the presence and absence of various ROS/RNS species.

fluorescence intensity of probe 1 have increased remarkably with a virtually unchanged peak position upon excitation at 580 nm. Based on the triple signal-to-noise ratio, the detection limit of probe 1 for ˙OH is determined as 0.05 μmol L^{-1}. The good linear relationship between the fluorescence response and concentration of ˙OH was obtained with a 0.9911 correlation coefficient (Fig. S15, ESI†). The probe 1 could selectively detected ˙OH mainly because the lone pair electrons of P^{III} atoms of triphenylphosphine moiety of the BODIPY fluorophore could be oxidized to triphenylphosphine oxide P^V=O to form the compound OX-1. In fact, this speculation has been demonstrated by preparing independently the compound OX-1 using Fenton reaction as depicted in Scheme 1. By comparing ^{31}P NMR spectroscopy of OX-1 and probe 1, the chemical shift of phosphorus atoms were obviously different and was −14.26 ppm and 32.00 ppm, respectively (Fig. S16, ESI†). These results demonstrated that probe 1 could be used as a sensitive turn-on fluorescence sensor for detecting ˙OH with excellent selectivity.

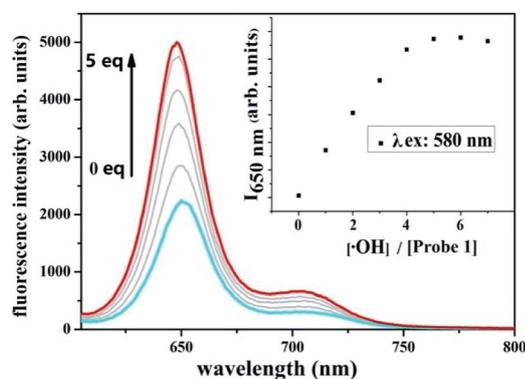### Practical application of probe 1

Having evaluated the ability of probe 1 to detect ˙OH in living cells, firstly, we checked its cytotoxicity by monitoring the survival rate of HeLa cells incubation with probe 1 after 5 h over a wide range of concentrations (0–200 μmol L^{-1}) according to the MTT viability assay (Fig. S17, ESI†). The results indicated that the HeLa cells maintained a high viability (>80%) after they had been incubated with 50 μmol L^{-1} probe 1, therefore, clearly could be used as intracellular luminescent probes. And then the ability of probe 1 to detect ˙OH was examined by using phorbol 12-myristate 13-acetate (PMA). In this experiment, HeLa cells were incubated with 10 μmol L^{-1} probe 1 for 30 min before PMA stimulation, and the fluorescence signal was very weak upon excitation at 633 nm (Fig. 4a and c). However, the fluorescence signal increased after PMA stimulation for 1 h (Fig. 4d and f). These results demonstrate that probe 1 can be used for detecting intracellular ˙OH.

Materials and methods

Reagents and instruments

3,4-Dihydroxybenzaldehyde, 1-bromohexadecane, boron trifluoride diethyletherate (BF$_3$·Et$_2$O), trifluoroacetic acid and 2-(diphenylphosphino)benzaldehyde were purchased from J&K Scientific Ltd. 2,4-Dimethyl-pyrrole was obtained from Nanjing Chemlin Chemical Industry Co. Ltd. Sodium hypochlorite (NaClO) and potassium dioxide (KO$_2$), tert-butyl hydroperoxide (TBHP) were supplied by Sigma Aldrich. Other chemicals or solvents were purchased from Sinopharm Chemical Reagent Co. Ltd, such as hydrogen peroxide (H$_2$O$_2$), ferric chloride hexahydrate (FeCl$_3$·6H$_2$O), ferrous sulfateheptahydrate (FeSO$_4$·7H$_2$O), N,N-dimethylformamide (DMF), dimethyl sulfoxide (DMSO), triethylamine (Et$_3$N), dichloromethane (CH$_2$Cl$_2$), et al. All chemicals and solvents were used directly without further purification unless otherwise noted. All air and moisture sensitive reactions were carried out under an argon
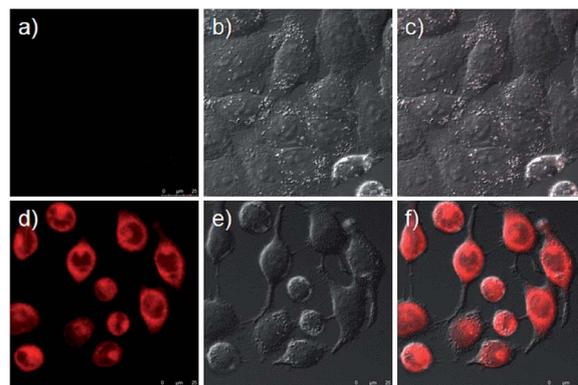

Fig. 3 Changes in the fluorescence spectrum of probe 1 (10 μmol L^{-1} in DMSO) as the concentration of ˙OH is increased upon excitation at 580 nm.

Fig. 4 Confocal fluorescence and bright field images of HeLa cells. (a) Cells incubated with 10 μmol L^{-1} of probe 1 for 30 min at 37 °C. (b) Bright field image of cells showed in (a). (c) One overlay image of (a and b). (d) Cells incubated with 10 μmol L^{-1} probe 1 at 37 °C for 30 min and then treated with PMA for 1 h. (e) Bright field image of cells showed in (d). (f) One overlay image of (d and e).

atmosphere. Dry CH_2Cl_2 was obtained by refluxing and distilling over CaH_2 under nitrogen. Triethylamine was obtained by simple distillation.

Nuclear magnetic resonance (NMR) spectra were obtained from a Bruker 500 or 600 MHz spectrometer with TMS as an internal standard operating for ^1H, ^{13}C NMR and ^{31}P NMR. Mass spectra were measured with a Bruker ultraflex MALDI TOF MS spectrometer. HRMS data were obtained on an Agilent 6224.

Procedures for ROS/RNS radicals sensing

Stock solutions of various ROS/RNS radicals (0.1 mol L^{-1}), such as H_2O_2, ClO^-, $O_2^{·-}$, TBHP, NO, NO_2^-, Vc, Fe^{3+}, GSH were prepared in deionized water. Fenton reaction between $FeCl_3$ and hydrogen peroxide was used to generate $^·OH$. For selectivity evaluation, probe **1** (3.0 mL, 10 μmol L^{-1}, dimethyl sulfoxide solution) was added to the quartz optical cell of 1 cm optical path length, and then, adding appropriate amounts of the ROS/RNS radicals sample. For titration, the $^·OH$ solution was gradually added to probe **1** (3.0 mL, 10 μmol L^{-1}, dimethyl sulfoxide solution) using a micro-pipette. Fluorescence was measured for 580 nm excitation within 585–800 nm.

Cell culture and fluorescence bioimaging

The HeLa cell line was provided by the Institute of Biochemistry and Cell Biology, SIBS, CAS (China). Cells were grown in high glucose Dulbecco's Modified Eagle Medium (DMEM, 4.5 g of glucose per L) supplemented with 10% fetal bovine serum (FBS) at 37 °C and 5% CO_2. Cells (5 × 108 L) were plated on 14 mm glass cover slips and allowed to adhere for 24 h. Experiments to assess $^·OH$ uptake were performed over 1 h in the same medium supplemented with 10 μmol L^{-1} phorbol 12-myristate 13-acetate (PMA). Immediately before the experiments, cells were washed with PBS buffer and then incubated with 10 μmol L^{-1} probe **1** in PBS buffer for 30 min at 37 °C. Cell imaging was then carried out after washing the cells with PBS buffer. Confocal fluorescence imaging was performed with a Zeiss LSM 710 laser scanning microscope and a 63× oil-immersion objective lens. Cells incubated with probe **1** were excited at 633 nm using a multi-line argon laser.

Experiments

Synthesis of compound 3

3,4-Dihydroxybenzaldehyde (1.38 g, 10 mmol), 1-bromohexadecane (12.2 g, 40 mmol), potassium carbonate (4.14 g, 30 mmol), potassium iodide (0.10 g, 0.6 mmol) and DMF (50 mL) were added to into a 100 mL flask, the mixture was then stirred at 70 °C for 14 h. After reaction completion, the mixture were cooled to room temperature and poured into ice water (100 mL). Then, solid precipitation was filter and recrystallized with a solvent mixture of chloroform and methanol to give gray solid product **3** in 83.6% yield (4.9 g).[34] ^1H NMR (CDCl$_3$, 500 MHz) δ (ppm): 9.83 (s, 1H), 7.44–7.39 (m, 2H), 6.95 (d, J = 10 Hz, 1H), 4.07 (q, J = 5 Hz, 4H), 1.90–1.80 (m, 4H), 1.54–1.41 (m, 4H), 1.40–1.16 (m, 48H), 0.88 (t, J = 10 Hz, 6H).

Synthesis of compound 2

In a 250 mL flask, a solution of compound **3** (1.17 g, 2 mmol) and 2,4-dimethylpyrrole (0.38 g, 4 mmol) in anhydrous CH_2Cl_2 (100 mL) was stirred under an atmosphere of argon for 10 min. Trifluoroacetic acid (0.01 mL) was added and the reaction mixture was stirred at room temperature overnight. 2,3-Dichloro-5,6-dicyano-1,4-benzoquinone (0.45 g, 2 mmol) was then added to the above mixture and stirred at room temperature for 1 h. The solution was cooled in an ice bath (0 °C) and the triethylamine (3.0 mL) and excessive $BF_3·Et_2O$ were added dropwise and the final mixture continually reacted at 0 °C for 5 h. The reaction was then quenched with water (30 mL) and the reaction mixture was worked up by extraction with CH_2Cl_2 (3 × 30 mL). The organic extract was dried by anhydrous Na_2SO_4, filtered, and rotary evaporated. The residue was purified by column chromatography over silica gel with a solvent mixture of petroleum ether/CH_2Cl_2 (v/v = 1/2) as the eluent to give compound **2** in 62.2% yield as a red solid. ^1H NMR (CDCl$_3$, 600 MHz): 6.97 (d, J = 6 Hz, 1H), 6.79–6.75 (m, 2H), 5.98 (s, 2H), 4.04 (t, J = 6 Hz, 2H), 3.94 (t, J = 6 Hz, 2H), 2.55 (s, 6H), 1.89–1.83 (m, 2H), 1.82–1.78 (m, 2H), 1.48 (s, 6H), 1.47–1.36 (m, 4H), 1.34–1.22 (m, 48H), 0.88 (t, J = 6 Hz, 6H). ^{13}C NMR (CDCl$_3$, 150 MHz) δ (ppm): 155.25, 149.72, 149.59, 143.22, 141.88, 131.75, 127.10, 121.03, 120.39, 113.75, 113.29, 69.45, 69.22, 31.94, 29.73, 29.68, 29.65, 29.64, 29.63, 29.61, 29.50, 29.44, 29.38, 29.28, 29.22, 26.06, 25.97, 22.71, 14.58, 14.46, 14.14. HRMS (ESI): m/z calcd for $C_{51}H_{84}BF_2N_2O_2$: 805.65884 $[M + H]^+$; found: 805.65775.

Synthesis of probe 1

Compound **2** (0.08 g, 0.1 mmol) and 2-(diphenylphosphino)benzaldehyde (0.11 g, 0.3 mmol) were added to a 100 mL two-neck round bottomed flask containing a 60 mL mixed solvent of acetonitrile and 1,2-dichloroethane (v/v = 3/1), and to this solution was piperidine (0.4 mL) and acetic acid (0.4 mL). The mixture was heated at 90 °C under Ar atmosphere by using a Dean–Starktrap, and the reaction was monitored by TLC. When compound **2** was completely consumed, the reaction mixture was cooled to room temperature and solvent was evaporated. Water (20 mL) was added to the residue and extracted with CH_2Cl_2 (3 × 20 mL). The organic phase was dried over anhydrous Na_2SO_4, filtered, and rotary evaporated. The residue was purified by column chromatography over silica gel with a solvent mixture of ethyl acetate/CHCl$_3$ (v/v = 1/3) as eluent to give probe **1** in 7.4% yield as a black solid. ^1H NMR (500 MHz, CDCl$_3$) δ (ppm): 8.04 (s, 1H), 8.01 (s, 1H), 7.95 (q, J = 5 Hz, 2H), 7.70–7.61 (m, 4H), 7.53 (t, J = 5 Hz, 1H), 7.49–7.44 (m, 2H), 7.42 (t, J = 5 Hz, 2H), 7.35–7.28 (m, 15H), 7.21 (t, J = 5 Hz, 2H), 6.95 (d, J = 5 Hz, 1H), 6.89 (q, J = 5 Hz, 2H), 6.77–6.73 (m, 2H), 6.44 (s, 2H), 4.04 (t, J = 5 Hz, 2H), 3.93 (t, J = 5 Hz, 2H), 1.89–1.83 (m, 2H), 1.82–1.77 (m, 2H), 1.48 (s, 6H), 1.45–1.39 (m, 4H), 1.30–1.22 (m, 48H), 0.90–0.85 (m, 6H). ^{13}C NMR (CDCl$_3$, 125 MHz) δ (ppm): 152.52, 149.61, 142.24, 140.91, 140.82, 139.23, 136.43, 136.28, 136.21, 134.27, 134.03, 133.87, 133.72, 133.63, 131.92, 129.22, 128.24, 128.64, 128.48, 127.51, 127.15, 126.33, 120.75, 120.55, 117.99, 113.68, 113.60, 69.54, 69.23, 31.93, 29.72, 29.68, 29.64, 29.50, 29.44, 29.37, 29.28, 29.23, 26.06, 25.97, 22.69, 14.66, 14.57, 14.12. ^{31}P NMR (202 MHz,

CDCl₃) δ (ppm): −14.26; MALDI-TOF MS: m/z: calculated for $C_{89}H_{110}BF_2N_2O_2P_2$ [M + H]⁺: 1349.8098; found: 1349.3503.

Synthesis of compound OX-1

In a 100 mL round bottomed flask, a solution of probe **1** (0.02 mmol) and hydrogen peroxide (0.2 mmol) in tetrahydrofuran (50 mL) were stirred at room temperature for 2 min. FeSO₄·7H₂O (0.12 mmol) was then added to this mixture. The final mixture was continually stirred at room temperature and ended until the probe **1** was completely consumed (monitored by TLC). After the solvent was evaporated, water (20 mL) was added to the residue and extracted with CHCl₃ (3 × 20 mL). The organic phase was dried over anhydrous Na₂SO₄, filtered, and evaporated to give compound **OX-1** in quantitative yield as a black solid. ¹H NMR (500 MHz, CDCl₃) δ (ppm): 8.14 (s, 1H), 8.10 (s, 1H), 8.04 (q, J = 5 Hz, 2H), 7.69–7.65 (m, 9H), 7.60–7.56 (m, 3H), 7.54–7.50 (m, 5H), 7.49–7.43 (m, 9H), 7.17 (q, J = 5 Hz, 2H), 6.94 (d, J = 5 Hz, 1H), 6.75–6.72 (m, 2H), 6.27 (s, 2H), 4.03 (t, J = 5 Hz, 2H), 3.93 (t, J = 5 Hz, 2H), 1.89–1.83 (m, 2H), 1.82–1.78 (m, 2H), 1.53–1.46 (m, 4H), 1.44 (s, 6H), 1.29–1.24 (m, 48H), 090–0.85 (m, 6H). ¹³C NMR (CDCl₃, 125 MHz) δ (ppm): 152.29, 149.73, 142.41, 141.34, 141.29, 139.70, 134.13, 134.11, 133.91, 133.83, 133.73, 133.27, 132.44, 132.31, 131.95, 131.00, 130.20, 128.69, 128.60, 127.66, 127.57, 127.02, 121.49, 120.12, 118.51, 113.77, 113.58, 69.52, 69.28, 31.94, 29.73, 29.50, 29.38, 29.29, 26.07, 26.00, 22.70, 14.58, 14.13. ¹⁴B NMR (160 MHz, CDCl₃) δ (ppm): 1.16; ³¹P NMR (202 MHz, CDCl₃) δ (ppm): 32.00; MALDI-TOF MS: m/z: calculated for $C_{89}H_{108}BFN_2O_4P_2$ [M − H − F]: 1360.8; found: 1360.5. HRMS (ESI): m/z calcd for $C_{89}H_{110}BF_2N_2O_4P_2$: 1381.79965 [M + H]⁺; found: 1381.80110.

Conclusions

In summary, we have successfully designed and synthesis a sensitive fluorescent probe to monitor ˙OH in living cells. This probe is designed based on BODIPY platform with two triphenylphosphine groups as a reactive-site. The probe's turn-on mechanism utilized an oxidation reaction of phosphorus atom by ˙OH. We envision that this probe may be a useful tool for investigation of physiological and pathological functions of ˙OH.

Conflicts of interest

There are no conflicts to declare.

Acknowledgements

Notes and references

1 W. R. Haag and C. C. D. Yao, *Environ. Sci. Technol.*, 1992, **26**, 1005–1013.

2 D. S. Pines and D. A. Reckhow, *Environ. Sci. Technol.*, 2002, **36**, 4046–4051.

3 A. Medel, J. Treviño-Reséndez, E. Brillas, Y. Meas and I. Sirés, *Electrochim. Acta*, 2020, **331**, 135382.

4 Z. Huang, P. Ying, L. Huang, Q. Xu and X.-Y. Hu, *Anal. Methods*, 2019, **11**, 5126–5133.

5 J. L. Cleveland and M. B. Kastan, *Nature*, 2000, **407**, 309–311.

6 Y. Yang, J. Zhou, Y. Zhang, Q. Zou, X. Zhang and J. Chen, *Sens. Actuators, B*, 2013, **182**, 504–509.

7 F. Scholz, G. López de Lara Gonzláez, L. Machado de Carvalho, M. Hilgemann, K. Z. Brainina, H. Kahlert, R. S. Jack and D. T. Minh, *Angew. Chem., Int. Ed.*, 2007, **46**, 8079–8081.

8 T. Oka, S. Yamashita, M. Midorikawa, S. Saiki, Y. Muroya, M. Kamibayashi, M. Yamashita, K. Anzai and Y. Katsumura, *Anal. Chem.*, 2011, **83**, 9600–9604.

9 T. Watanable, M. Yoshida, S. Fujiwara, K. Abe, A. Onoe, M. Hirota and S. Igarashi, *Anal. Chem.*, 1982, **54**, 2470–2474.

10 Y. Cao, D. Sui, W. Zhou and C. Lu, *Sens. Actuators, B*, 2016, **225**, 600–606.

11 G. Cui, Z. Ye, J. Chen, G. Wang and J. Yuan, *Talanta*, 2011, **84**, 971–976.

12 Y. Xu, D. Wang, Y. Zhang, J. Zhang, S. Jiang, W. Liang, T. Zhu and B.-C. Ye, *Anal. Chim. Acta*, 2020, **1096**, 69–75.

13 T.-T. Wang, Z.-L. Huang, Q. Xu and X.-Y. Hu, *Int. J. Environ. Anal. Chem.*, 2018, **98**, 477–491.

14 Y. Huang, A. Sinha, H. Zhao, X. Dang, Y. Zhang and X. Quan, *ChemistrySelect*, 2019, **4**, 12507–12511.

15 R. Zhang, J. Zhao, G. Han, Z. Liu, C. Liu, C. Zhang, B. Liu, C. Jiang, R. Liu, T. Zhao, M.-Y. Han and Z. Zhang, *J. Am. Chem. Soc.*, 2016, **138**, 3769–3778.

16 F. Liu, J. Du, D. Song, M. Xu and G. Sun, *Chem. Commun.*, 2016, **52**, 4636–4639.

17 X. Bai, Y. Huang, M. Lu and D. Yang, *Angew. Chem., Int. Ed.*, 2017, **56**, 12873–12877.

18 D. Andina, J.-C. Leroux and P. Luciani, *Chem.–Eur. J.*, 2017, **23**, 13549–13573.

19 L. Zeng, T. Xia, W. Hu, S. Chen, S. Chi, Y. Lei and Z. Liu, *Anal. Chem.*, 2018, **90**, 1317–1324.

20 J.-Y. Wang, Z.-R. Liu, M. Ren, X. Kong, K. Liu, B. Deng and W. Lin, *Sens. Actuators, B*, 2016, **236**, 60–66.

21 O. Adegoke and P. B. C. Forbes, *Anal. Chim. Acta*, 2015, **862**, 1–13.

22 W. Zhou, Y. Cao, D. Sui and C. Lu, *Angew. Chem., Int. Ed.*, 2016, **55**, 4236–4241.

23 X. Hai, Z. Guo, X. Lin, X. Chen and J. Wang, *ACS Appl. Mater. Interfaces*, 2018, **10**, 5853–5861.

24 T. T. Chen, Y. H. Hu, Y. Cen, X. Chu and Y. Lu, *J. Am. Chem. Soc.*, 2013, **135**, 11595–11602.

25 P. Kaur and K. J. Singh, *J. Mater. Chem. C*, 2019, **7**, 11361–11405.

26 D. Wu, L. Chen, W. Lee, G. Ko, J. Yin and J. Yoon, *Coord. Chem. Rev.*, 2018, **354**, 74–97.

27 H. Lu, J. Mack, Y. Yang and Z. Shen, *Chem. Soc. Rev.*, 2014, **43**, 4778–4823.

28 X. Qu, Q. Liu, X. Ji, H. Chen, Z. Zhou and Z. Shen, *Chem. Commun.*, 2012, **48**, 4600–4602.

29 J. Yang, F. Cai, N. Desbois, L. Huang, C. P. Gros, F. Bolze, Y. Fang, S. Wang and H. Xu, *Dyes Pigm.*, 2020, **175**, 108173.

30 J. Yang, H. Jiang, N. Desbois, G. Zhu, C. P. Gros, Y. Fang, F. Bolze, S. Wang and H. Xu, *Dyes Pigm.*, 2020, **176**, 108183.

31 L. Jean-Gérard, W. Vasseur, F. Scherninski and B. Andrioletti, *Chem. Commun.*, 2018, **54**, 12914–12929.

32 K. Lei, M. Sun, L. Du, X. Zhang, H. Yu, S. Wang, T. Hayat and A. Alsaedi, *Talanta*, 2017, **170**, 314–321.

33 X. Qu, W. Song and Z. Shen, *Front. Chem.*, 2019, **7**, 598.

34 M. Li, H. Xu, Y. Yang, L. Zhao, Z. Shen, Q. Zeng and C. Wang, *Chem. Lett.*, 2014, **43**, 1764–1766.